INTERNATIONAL JOURNAL OF CURRENT RESEARCH IN CHEMISTRY AND PHARMACEUTICAL SCIENCES
(p-ISSN: 2348-5213: e-ISSN: 2348-5221)
www.ijcrcps.com
(A Peer Reviewed, Referred, Indexed and Open Access Journal)
DOI: 10.22192/ijcrcps Coden: IJCROO(USA) Volume 13, Issue 2- 2026

Research Article

DOI: http://dx.doi.org/10.22192/ijcrcps.2026.13.02.003

In-vivo anti-nociceptive and anti-inflammatory potentials and molecular docking evaluation of chemical constituents of *Dioscorea praehensilis* targeting Cyclooxygenase-2 and chemokine receptor type 2 inhibition

Iyabo Mobolawa Adebisi[1], Aliyu Hamidu Ahmed[2], Boniface Clement Gomo[3], Sunday Joseph Fajobi[4], Taiwo Oladehinde[5], Samuel Jacob Bunu[6]

[1]Department of Pharmacology and Toxicology, Faculty of Pharmaceutical Sciences, Usmanu Danfodiyo University, Sokoto. Nigeria
[2]Department of Pharmacognosy and Ethnopharmacy, Faculty of Pharmaceutical Sciences, Usmanu Danfodiyo University, Sokoto. Nigeria.
[3]Department of Biochemistry and Molecular Biology, Federal University, Birnin Kebbi, Nigeria.
[4]Department of Physiology and Pharmacology, SUNY Downstate Health Sciences University, Brooklyn, New York, USA.
[5]Department of Biochemistry, Faculty of Biological Sciences, Adekunle Ajasin University, Akungba Akoko, Nigeria.
[6]Department of Pharmaceutical and Medicinal Chemistry, Faculty of Pharmacy, Niger Delta University, Bayelsa, Nigeria.
*Corresponding author: Email: *iyabo.adebisi@udusok.edu.ng*

Abstract

Dioscorea praehensilis has ethnobotanical applications in treating inflammation. This study assessed the anti-nociceptive and anti-inflammatory effects of *D. praehensilis* methanol extract using in vivo models, including the tail-flick, hot-plate, and formalin-induced paw oedema tests in rats, as well as in silico analysis. Bioactive compounds identified by HPLC in *D. praehensilis* were subjected to molecular docking with the X-ray crystal structures of cyclooxygenase-2 and chemokine receptor type-2. In the tail-flick and hot-plate models, administration of 50, 100, and 200 mg/kg *D. praehensilis* produced a dose-dependent increase in latency 60 min post-treatment. In the formalin test, *D. praehensilis* at 200 mg/kg significantly inhibited rat paw oedema during the third and fourth hours post-administration. Rutin, hesperidin, epicatechin, phytic acid, and catechin were the top five compounds against cyclooxygenase-2, with docking scores ranging from -9.4 to -7.3 kcal/mol. In contrast, kaempferol, rutin, catechin, hesperidin, and epicatechin ranked highest for chemokine receptor type-2 protein (docking scores -7.9 to 6.9 kcal/mol). The tested compounds were predicted to exhibit acceptable pharmacokinetic and safety profiles. These findings suggest that *D. praehensilis* possesses analgesic and anti-inflammatory properties, indicating its promise as a source of new therapeutic agents.

Keywords: *Dioscorea prehensilis,* antinociceptive, anti-inflammatory, Cyclooxygenase-2, chemokine receptor type-2, Molecular docking

Introduction

Pain, defined as a distressing sensory and emotional experience caused by actual or potential tissue damage, is a major reason for seeking medical care (Kumar and Elavarasi, 2016; Sisignano *et al.*, 2025). It is generally triggered by noxious stimuli and transmitted to the central nervous system via highly specialised neuronal networks (Yam *et al*., 2018). Affected neurons convey the pain signal to the spinal cord, which then relays it to the brain for processing (Alhassen *et al*., 2021). Most diseases encountered in modern medicine are accompanied by pain; hence, it is a global public health concern and a leading cause of disability worldwide (Uritu *et al*., 2018).

Conversely, inflammation is an important physiological process that protects the body from potentially harmful substances, including infections, dust, toxic chemicals, physical injuries, and tumour growth (Sokeng *et al*., 2020; Wang *et al*., 2021). As a natural defence mechanism, it aids in removing irritants and invading organisms, while also producing chemical mediators that facilitate the healing of damaged tissues and recruit migratory cells (Yusof *et al*., 2019; Paradee *et al*., 2021). However, uncontrolled inflammation can generate neurotoxic factors that worsen underlying disease conditions and lead to chronic inflammatory diseases such as gastric ulcers, diabetes, cardiovascular disease, cancer, autoimmune disorders, and neurodegenerative diseases (Paradee *et al*., 2021; Wang *et al*., 2021). The chemokine receptor type 2, a cell surface receptor, plays a crucial role in recruiting monocytes to sites of inflammation and guiding their differentiation into macrophages or dendritic cells (Chu *et al*., 2014). Cyclooxygenase-2 (COX-2), on the other hand, is an enzyme released at the site of tissue injury, which stimulates the production of prostaglandin E2 (PGE2), a hormone-like substance that causes pain and inflammation (Desai *et al*., 2018). Despite the availability of effective drugs, pain and inflammation remain persistent and serious health problems, affecting 80% of the adult population worldwide (WHO, 2012). Widely used pain control medications such as non-steroidal anti-inflammatory drugs (NSAIDs) and opioids are often misused and have significant side effects.

For example, NSAID use is limited by multiple adverse effects, including gastric bleeding, nephrotoxicity, hepatotoxicity, and cardiovascular issues (Han *et al*., 2025). Opioids could cause nausea, vomiting, respiratory depression, dependence, and tolerance (Katzung, 2017). Currently, the potential of COX-2 inhibitors as analgesic and anti-inflammatory agents that lack the gastrointestinal side effects associated with traditional NSAIDs is under active investigation. There is evidence that some of these agents have significant adverse effects and concerns about cardiovascular and liver toxicity, which has led to the withdrawal of most COX-2 selective agents from the market. There is therefore a need to search for agents of natural origin with a better safety profile (Hong *et al*., 2024; Takeda and Sashide, 2025).

Dioscorea praehensilis is a member of the Dioscoreaceae family. Ethnobotanical uses have been reported for the treatment of inflammation and scorpion bites. Previous studies showed that it reduced systolic blood pressure and mean albumin-creatinine ratio in a rat model of preeclampsia (Adebisi *et al*., 2018[a]). The methanol extract of its rhizome has also been shown to inhibit platelet aggregation (Adebisi *et al*., 2018[b]). In another study, purified tyrosinase from *D. praehensilis* facilitated the conversion of soluble proteins into fibrous protein networks. The enzyme was covalently linked to bovine serum albumin (BSA) to form a tyrosinase-BSA adduct, suggesting that yam tyrosinase is a useful enzyme in biotechnology (Ilesanmi *et al*., 2021). A recent study demonstrated the wound-healing properties of its methanol extract (Adebisi *et al*., 2025). In the present study, we investigated the antinociceptive and anti-inflammatory activities of *D. praehensilis* using animal and *in silico* models.

Materials and Methods

Chemicals and Drugs

Piroxicam injection (Feldene®) by NeimethInternational Pharmaceuticals Plc. was obtained from a local pharmacy premise. Formalin (Sigma-Aldrich) was obtained from the research laboratory of Pharmacology and Toxicology at the Faculty of Pharmaceutical Sciences, Usmanu Danfodiyo University, Sokoto.

Experimental Animals

Female Sprague–Dawley rats (180-210 g) and mice (21-25 g) were purchased from the animal house of the Department of Pharmacology, Ahmadu Bello University, Zaria. The animals were housed under controlled conditions of temperature (23±2 °C), humidity (55±10 %), and lighting (12-h light/dark cycle), and provided with food and water *ad libitum*. Animals were acclimated for 2 weeks after arrival. All experiments were conducted in accordance with the institution's guidelines for the care and use of laboratory animals in research, with ethics approval number PTAC/Dp/(Me)OT/37-21.

Preparation of Plant Materials and Extraction

The rhizome of *D.praehensilis* was collected in Sokoto in August 2022, identified and authenticated by a consultant taxonomist to the herbarium of the Department of Pharmacognosy and Ethnomedicine, Faculty of Pharmaceutical Sciences, Usmanu Danfodiyo University, Sokoto. The voucher specimen has been deposited in the herbarium unit (PCG/UDUS/Dios/0002). The plant material was then air-dried in the shade to constant weight and size-reduced to a fine powder using a mortar and pestle. The powdered material was then extracted by maceration with 80% methanol for 3 days. The resulting extract was evaporated to dryness using a water bath controlled at 45°C.

Analgesic Studies

Tail Flick Test

The analgesic activity of the extract was evaluated using the tail-flick method described by D'amour and Smith (1941). Female mice were divided into 5 groups of 5 mice each. One to 2 cm of the mouse tail was immersed in warm water maintained at 55 ± 0.5°C. The reaction/latency

time (in seconds) was defined as the time taken by the mouse to flick its tail in response to pain. A cutoff time of 15 seconds was used to avoid tail injury from heat. Mice were treated with distilled water (10 mL/kg, vehicle-treated control), piroxicam (10 mg/kg, positive control), and *D.praehensilis* extract (50, 100, and 200 mg/kg). The latency of the tail-flick response was determined at 20, 40, and 60 minutes after treatment.

Hot Plate Test

The analgesic activity of the extract was also evaluated using the hot-plate method described by Eddy and Leimback (1953). Rats were divided into five groups of 5 rats each. Rats were placed in a restrainer on a hot plate maintained at 55± 0.5 °C. Reaction time (latency) was measured as the time taken for the rats to respond to thermal pain by licking their paws or jumping. The maximum reaction time was set at 40 sec to prevent paw injury. Rats were treated with distilled water (10 mL/kg, vehicle-treated control), piroxicam (10 mg/kg, positive control), and D. praehensilis extract (50, 100, and 200 mg/kg). Tail-flick latency was determined at 20, 40, and 60 minutes after treatment.

Anti-inflammatory Study

Formalin-Induced Paw Oedema

The formalin-induced inflammation described by Winter *et al*. (1962) was used. Rats were divided into five groups of 5 rats each and treated with distilled water (vehicle-treated control), 10 mL/kg; piroxicam, 10 mg/kg (positive control); and *D. praehensilis* extract (50, 100, and 200 mg/kg). Oedema was induced in the right hind paws by a subplantar injection of 0.02 mL of 2.5% formalin 30 minutes after drug administration. Swelling of the formalin-injected foot was measured using a digital calliper (Skole®) hourly during the first and fifth hours after the formalin injection. The ability of the anti-inflammatory agents to suppress inflammation was expressed as a percentage inhibition of paw oedema and calculated according to the following equation:

Relative Paw Edema = (V2-V1/V1) *100

Where V1 = The animal paw volume before formalin injection

V2 = The paw volume after drug/extract treatment and formalin injection at different time points.

High-performance liquid chromatography analysis (HPLC)

The aqueous extract of *D. praehensilis* was subjected to HPLC analysis using Agilent 1100 dual binary pumps, an HP CTO-10AS column oven, and an HP Prominence SPD-20A UV/Vis detector to identify its bioactive constituents. Briefly, 0.2 g of the test sample was weighed into a test tube, and 15 mL of ethanol and 10 mL of 50% m/v potassium hydroxide were added. The mixture was kept in a water bath at 60 °C for 3 hours, then transferred to a separatory funnel and washed with 20 mL of ethanol, 10 mL of cold water, 10 mL of hot water, and 3 mL of hexane. The extracts were combined and washed three times with 10 mL of a 10% v/v ethanol aqueous solution, and the ethanol was then evaporated. The residue was solubilised in 1000 µL of pyridine, and 200 µL was transferred to a vial for HPLC analysis. The analysis was performed using a C-12 normal-phase column (Phenomenex Gemini 5 µ, 200 mm × 4.8 mm). The mobile phase consisted of acetic acid-acidified deionised water (pH 2.8) as solvent A and acetonitrile as solvent B at a flow rate of 0.8 mL/min. The column was equilibrated with 5% solvent B for 20 minutes after each sample injection. The column temperature was set to 38 °C, and the injection volume was 20 µL. The wavelength was set to 280 nm for phytochemical detection. Identification and quantification of phytochemicals were performed by comparing retention times and peak areas with those of pure standard compounds, utilising the external standard method to construct a calibration curve. Gradient elution was executed as follows: 0-5 min, 5-9% solvent B; 5-15 min, 9% solvent B; 15-

22 min, 9-11% solvent B; 22-38 min, 11-18% solvent B; 38-43 min, 18-23% solvent B; 43-44 min, 23-90% solvent B; 44-45 min, 90-80% solvent B; 45-55 min.

In silico studies

Molecular Docking

Fifteen (15) bioactive compounds identified by HPLC analysis from the *D. praehensilis* were selected and subjected to molecular docking analysis with the X-ray crystal structure of chemokine receptor type 2 (CCR2A) in complex with MK-0812 (PDB ID: 6GPS), (Apel *et al*., 2019) and crystal structure of uninhibited mouse cyclooxygenase-2 (COX-2) (i.eprostaglandin synthase-2) (PDB ID: 5COX), (Kurumbail *et al*., 1996) retrieved from the Protein Data Bank (PDB) (https://www.rcsb.org/). Celecoxib (a selective COX-2 inhibitor) was used as the standard control. The Maestro Molecular Modelling Suite 2020 (Schrödinger) was employed for ligand and target protein preparation. Bioactive compound simplified molecular input line entry system (SMILES) strings, sourced from PubChem, were converted into 3D structures using Maestro's LigPrep wizard. The crystallographic protein structures were processed with Maestro's protein preparation module: bond orders were assigned, water molecules located more than 5 Å from het groups were deleted, and het states were generated at default pH (7.0 ± 2.0) using Epik. Following this, a docking grid was generated with a bounding box encompassing the entire target site, using docking parameters 7.25, -12.54, -11.87 (6GPS) and 36.13, 34.80, 59.17 (5COX), respectively. Glide SP (Schrödinger) was then used to execute the docking simulations (Schrödinger, 2020).

Pharmacokinetic Studies

To estimate various *in silico* pharmacokinetic parameters, the ligands' chemical structures were submitted using the SMILES. The drugs' pharmacokinetic profile was assessed using the Swiss ADME program (http://www.swissadme.ch). The parameters measured include Human gastrointestinal absorption (HIA), blood-brain barrier (BBB) permeation, the interaction of molecules with cytochromes P450 (CYP), the bioavailability score, and the readout of the BOILED-Egg model substrate or non-substrate of the permeability glycoprotein (P-gp) (Daina *et al*., 2017).

Prediction of Toxicity

The Protox 3 server was used to predict the organ toxicities and toxicological endpoints of the ligands, including their LD_{50} values. The integrated PubChem search (https://pubchem.ncbi.nlm.nih.gov) was used to retrieve chemical structures from compound names. The models to be used were selected, and the web server computed the acute toxicity and the selected toxicity targets (Banerjee *et al*., 2024).

Statistical Analysis

Data were presented as mean ± standard error of the mean (SEM). The results were analysed using GraphPad Prism version 8 software. Multiple comparisons of means amongst groups were made using one-way analysis of variance (ANOVA), and Dunnett's post-test comparison was used to test for statistically significant differences at $p< 0.05$

Results

Analgesic Studies

Tail flick test

At 20 minutes post-administration, there was an insignificant increase in reaction time across all treatment groups compared to the control. However, at 40 minutes post-administration, a significant increase in reaction time occurred in a dose-dependent manner ($p<0.01$). Similarly, a dose-dependent increase in reaction time was observed at 60 min post-administration in all treatment groups ($p<0.05$ at 50, 100 mg/kg DP, and 10 mg/kg piroxicam; $p<0.001$ at 200 mg/kg DP) (Figure 1).

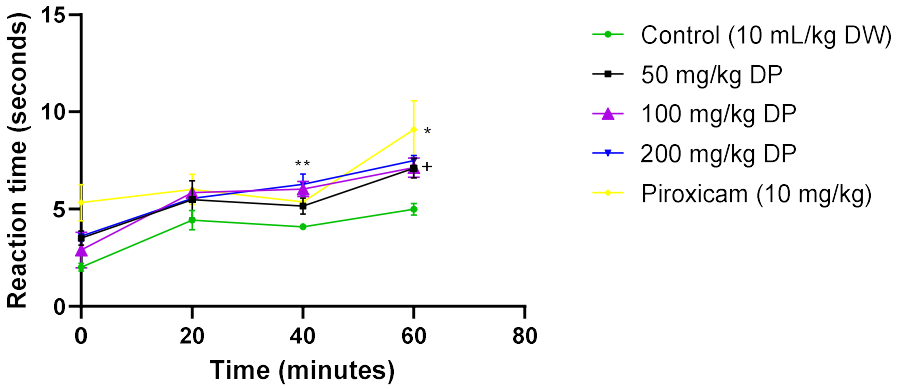

Figure 1: Effect of the methanol extract of *D. praehensilis* on the tail flick test in mice. Data are presented as mean± SEM. ** P<0.01, * P<0.05, $^{+}$ P<0.001, DP= *Dioscoreapraehensilis*, DW= Distilled water. N=5.

Hot plate test

At 20 min post-administration, there was a significant dose-dependent increase in the reaction time in the groups treated with 100 and 200 mg/kg DP (p<0.01). Similarly, at 40 mins post-administration, the reaction time in all treatment groups was significantly longer than in the control (p<0.01). Furthermore, at 60 min post-administration, a significant increase was observed in all treatment groups compared with the vehicle-treated control (p<0.001 at 50 and 100 mg/kg DP; p<0.0001 at 200 mg/kg DP) (Figure 2). Compared with the standard drug, no significant difference was observed between the groups that received 100 and 200 mg/kg DP during the latent period (i.e.,p > 0.05).

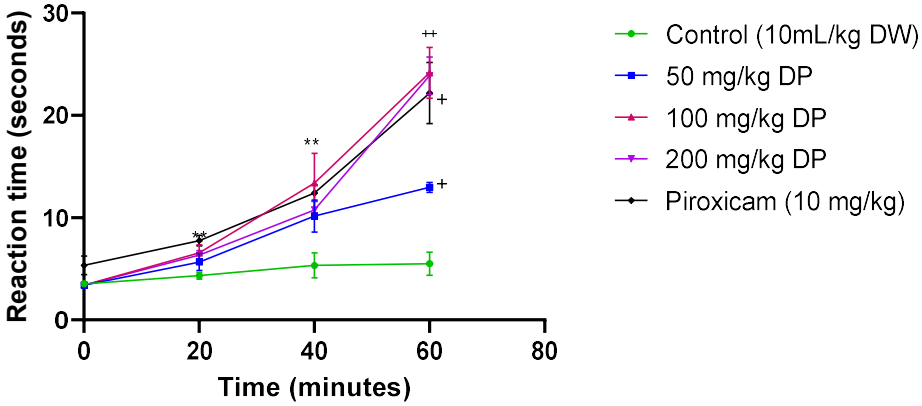

Figure 2: Effect of the methanol extract of *Dioscoreapraehensilis* on the hot plate test in rats. Data are presented as mean± SEM. ** P<0.01, $^{+}$P<0.001, $^{++}$ P<0.0001, DP= *Dioscoreapraehensilis*, DW= Distilled water. N=5.

Anti-inflammatory Study

The results showed that 200 mg/kg DP significantly (p<0.05) inhibited formalin-induced rat paw oedemaat the third and fourth hours compared with the vehicle-treated group. Also, there was no significant difference between 200 mg/kg of the extract andthe standard drug in inhibiting formalin-induced swelling (p> 0.05)

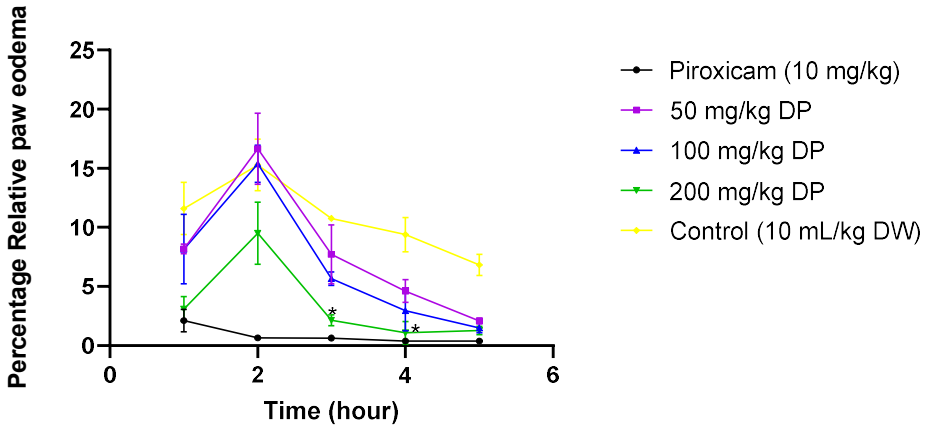

Figure 3: Comparison of the reduction of formalin-induced paw oedema in rats treated with vehicle, piroxicam, and *D. praehensilis*. Data are presented as mean± SEM *P<0.05, DP= *Dioscoreapraehensilis*, DW= Distilled water. N=5.

HPLC analysis

The HPLC analysis of the aqueous extract of *D.praehensilis* revealed the presence of fifteen (15) compounds. The major compounds include oxalate, sapogenin, phytic acid, epicatechin, quabain, and kaempferol. The comprehensive list of compounds is presented in Table 1, and Figure 4 shows the chromatogram.

Table 1: Bioactive constituents of aqueous crude extract of *D. praehensilis* identified by HPLC

Compound	Retention	Area	Height	Concentration	Units
Lunamarin	0.203	4278.068	258.404	5.0109	µg/mL
Naringin	1.583	4698.6786	232.484	3.6805	µg/mL
Quabain	2.633	12106.27	597.691	12.3955	µg/mL
Flavan-3-ol	4.4	10108.439	501.549	5.8719	ppm
Naringenin	12.63	6367.8406	330.16	6.0544	µg/mL
Spartein	15.62	5348.1413	264.08	7.1884	µg/mL
Rutin	18.95	6366.3492	314.018	5.9259	µg/mL
Hesperidine	22.456	8543.8936	420.917	3.6638	Ppm
Steriods	25.563	4878.6482	240.809	6.2761	Ppm
Kaempferol	27.916	14482.375	685.935	10.0293	µg/mL
Epicatechin	28.256	8427.8389	472.013	12.6436	µg/g
Phytic acid	33.81	18145.624	885.941	20.3244	µg/mL
Oxalate	35.65	17287.042	848.794	24.0726	µg/mL
Catechin	36.526	5036.5803	252.472	1.548	µg/mL
Sapogenin	42.706	13246.946	651.09	21.7698	µg/mL

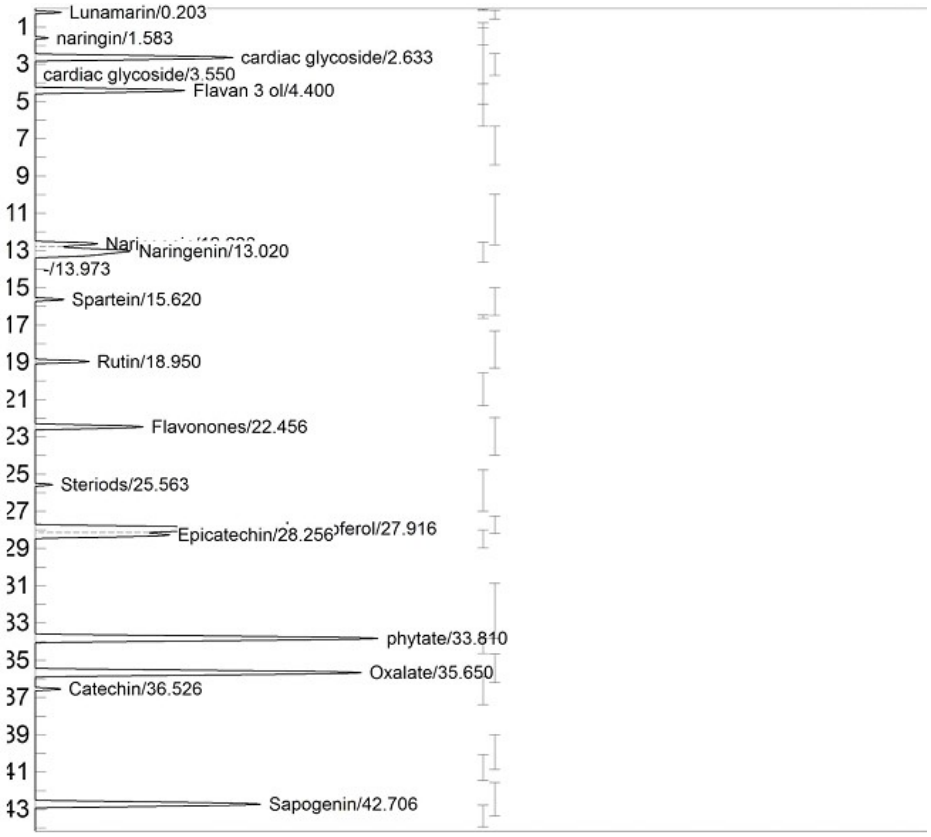

Figure 4: HPLC chromatogram of the compounds present in the aqueous extract of *D. prehensilis*

Molecular docking analysis

The molecular docking analysis revealed that the bioactive compounds of *D.praehensilis* exhibit varying binding affinities for the two target proteins.The top five (5) ranking compounds had binding affinities ranging from -9.4 to -7.3kcal/mol for Cycloxygenase-2 and from -7.9 to -6.9 kcal/mol for chemokine receptor type 2, while those of the standard ligand, celecoxib, were -6.4 and 5.5 kcal/mol,respectively. Tables 2 and 3 represent the PubChem CID, molecular formula, molecular weight, and docking scores of these top-ranking compounds against cycloxygenase-2 and chemokine receptor type 2, respectively, while Figure 5 shows their molecular structures. The entire list of the 15 compounds in *D. praehensilis*, along with their docking scores (kcal/mol) against Cycloxygenase 2 and chemokine receptor type 2, is available in Supplementary Table 1.

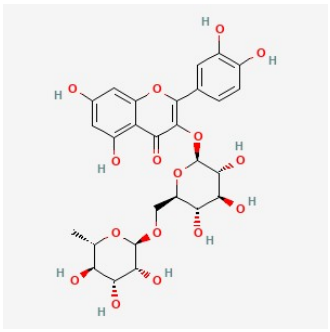

Rutin

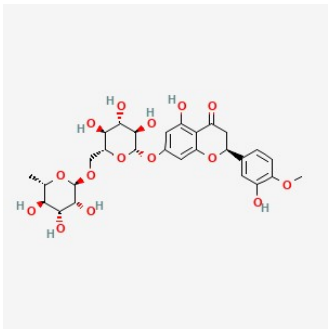

Hesperidin

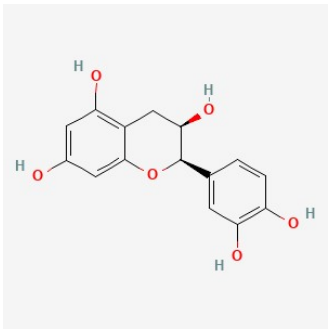

Epicatechin

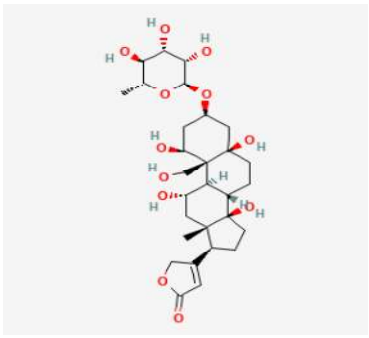

Ouabain

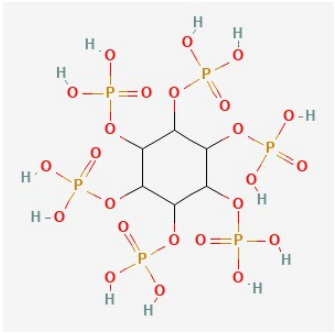

Phytate

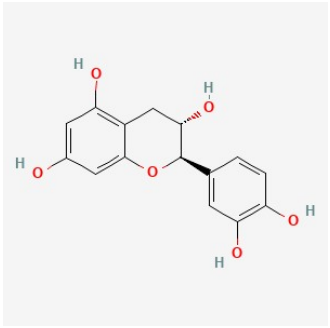

Catechin

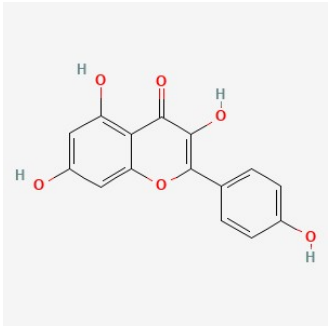

Kaempferol

Figure 5: Molecular structures of the top-ranking compounds from the methanol extract of *D. praehensilis*

The two-dimensional (2D) and three-dimensional (3D) interaction profiles of the amino acid moiety of 5COX with the top-selected compounds from *D. praehensilis* and the standard are displayed in Figure 6–11and Table 4. Analysis of the 2D and 3D interactions showed that the top-ranking compound, rutin, established seven hydrogen bonds with six amino acid residues in the proteinsequence. These hydrogen bonds were with ASN 144, SER 143, TRP 139, LYS 333, GLU 140 and ARG 222. Additionally, rutinformed 5 hydrophobic bonds with some amino acid residues, namely LEU145, PHE 142, TRP 139, LEU 238, and LEU 224, and 4 polar bonds with ASN 231, GLN 241, THR 237, and GLN 330. The second compound, hesperidin, conversely formed four hydrogen bonds with three amino residues, namely GLY 536, ARG 376 and GLU 236. It also established four hydrophobic, three polar and one pi-pi stacking bonds. Epicatechin, the third compound,formed six hydrogen bonds with five amino acid residues in the protein sequence: GLY 235, LYS 333, GLU 140, GLN 241, and SER 143. Other bonds associated with it include five hydrophobic and four polar bonds. The fourth compound, phytic acid, on the other hand,formed eight hydrogen bonds with eight amino acids in the protein. These include GLU 236, LYS 333, TRP 139, LEU 238, LEU 224, GLN 241, GLU 140 and LEU 145. Furthermore, it engaged three hydrophobic bonds, four polar bonds and one salt bridge with the protein sequence. The fifth compound, catechin,formed four hydrogen bonds with four amino acid residues, including GLY 235, GLN 241, GLU 140, and LEU 224. Furthermore, it created three hydrophobic and four polar bonds with some other residues in the sequence.

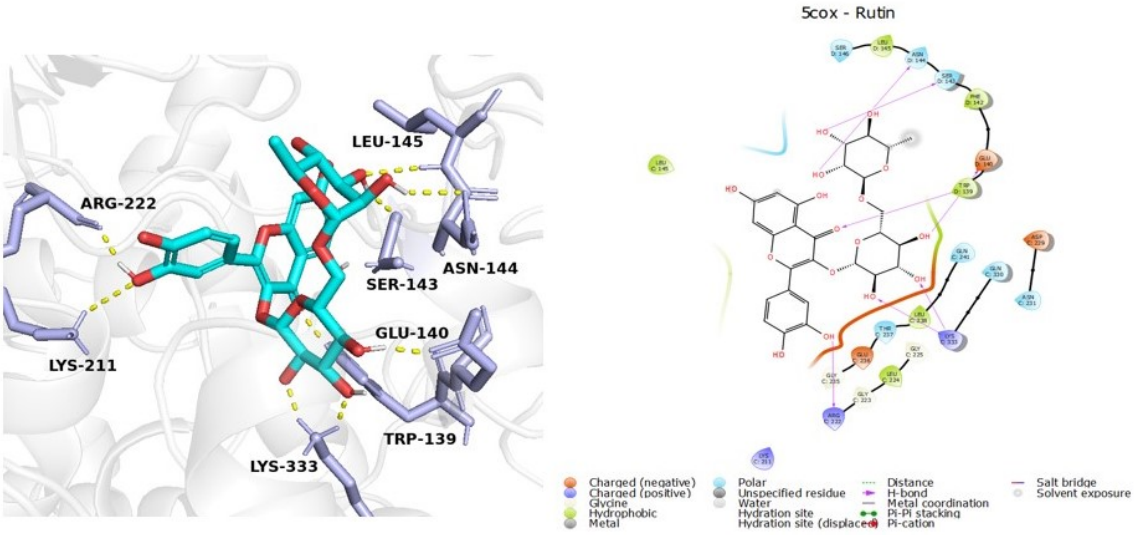

Figure 6: Molecular interaction of amino-acid residues of cyclooxygenase-2with Rutin. 3D left, 2D right.

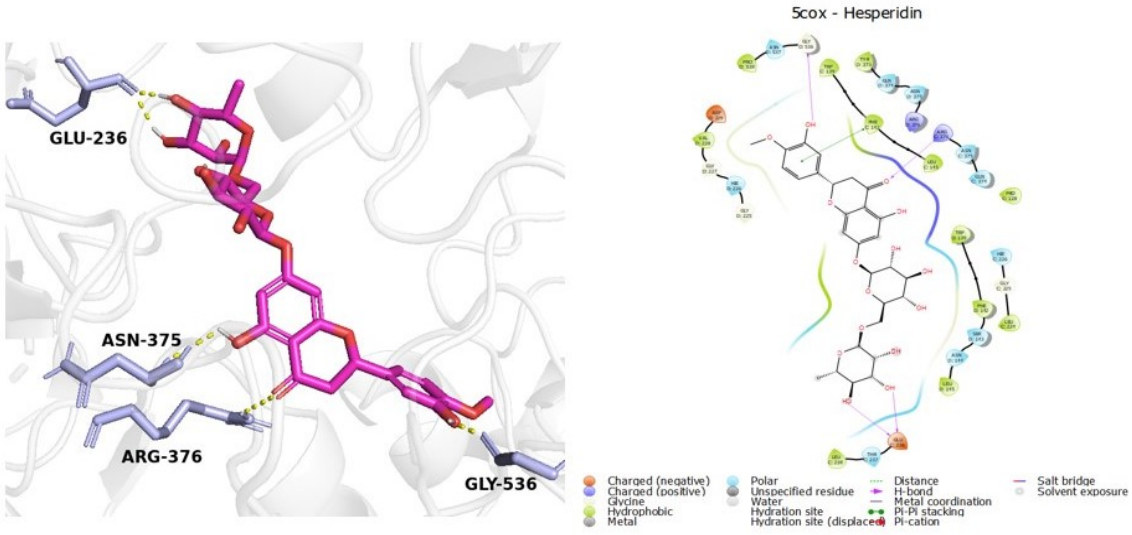

Figure 7: Molecular interaction of amino-acid residues of cyclooxygenase-2with Hesperidin. 3D left, 2D right.

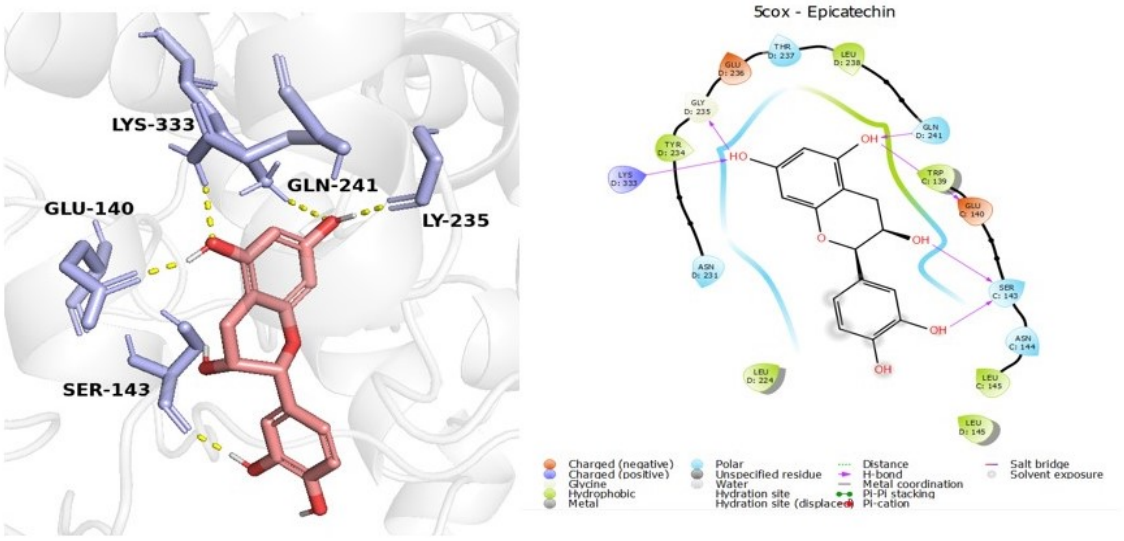

Figure 8: Molecular interaction of amino-acid residues of cyclooxygenase-2with Epicatechin 3D left, 2D right.

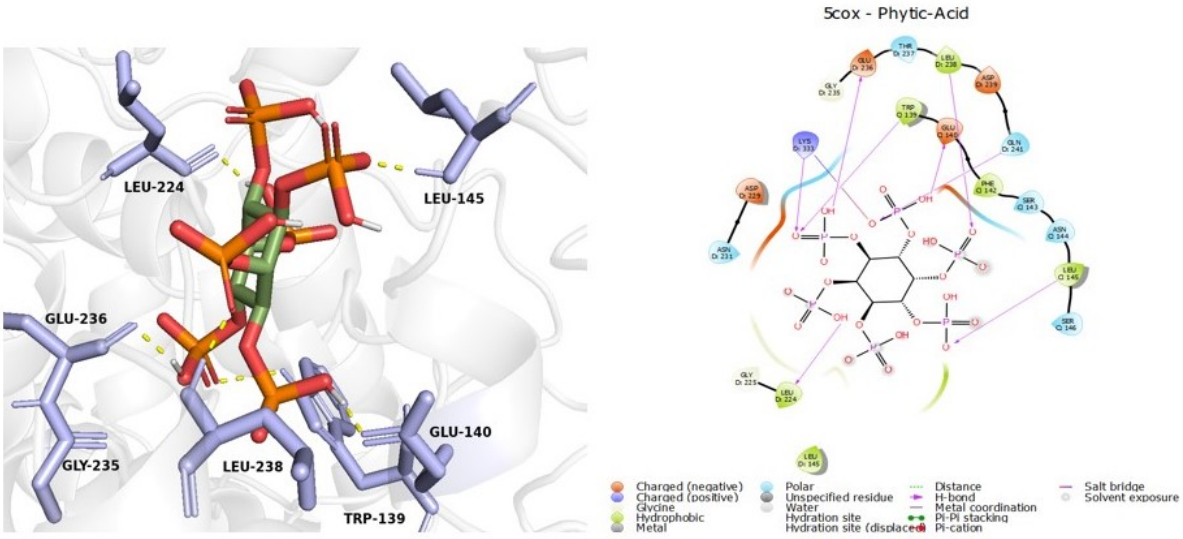

Figure 9: Molecular interaction of amino-acid residues of cyclooxygenase-2with Phytate. 3D left, 2D right.

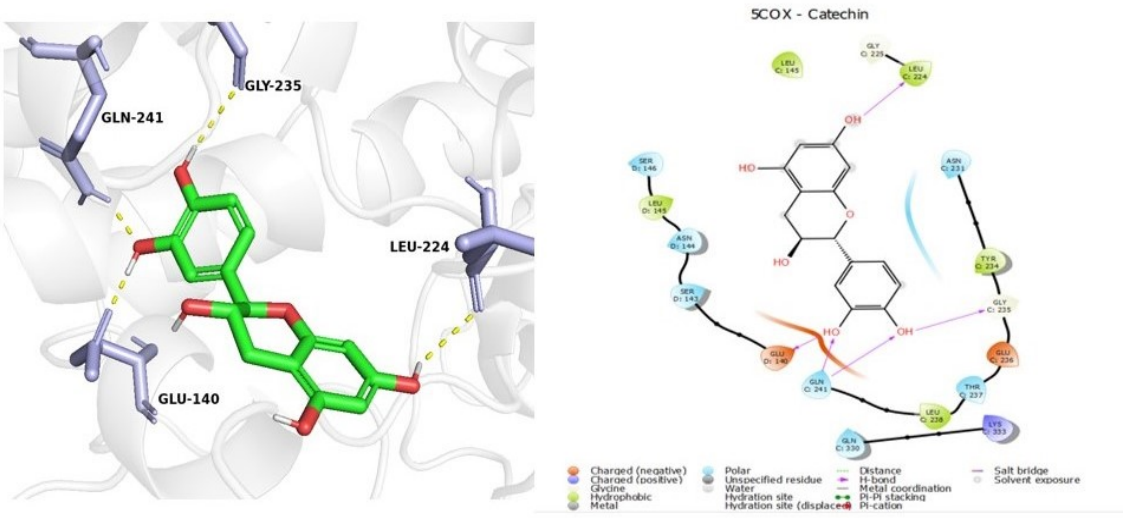

Figure 10: Molecular interaction of amino-acid residues of cyclooxygenase-2 with Catechin. 3D left, 2D right

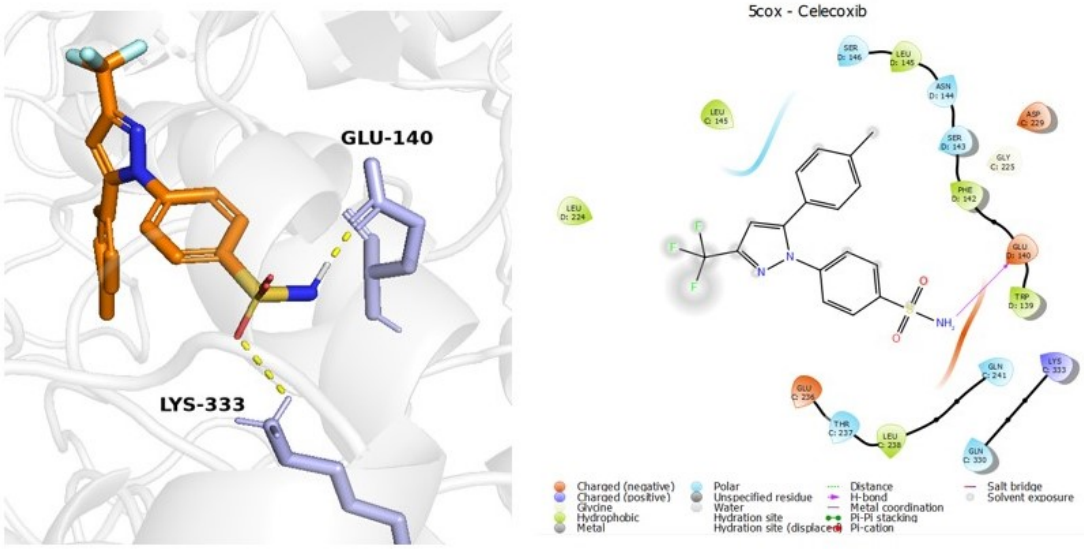

Figure 11: Molecular interaction of amino-acid residues of cyclooxygenase-2with the standard ligand (Celecoxib). 3D left, 2D right.

The 2D and 3D interactions of 6GPSwith the top selected compounds from *D.praehensilis* and the standard are displayed in Figures 12–17 and Table 5, while Figure 18 shows its interaction with the co-crystalised compound. The top-ranking ligand, kaempferol, interacted with amino acid residues in 6GPS by forming three hydrogen bonds. The residues involved include SER 101, GLU 291 and THR 179. Additional interactions of this ligand include the formation of three hydrophobic and polar bonds, each and one pi-pi stacking. The second ligand, rutin, conversely formed four hydrogen bonds. The amino acid residues involved include LYS 38, GLN 288, GLU 291 and SER 101. Similarly, catechin, hesperidin, and ouabain each formed 4 hydrogen bonds with

amino acid residues in 6GPS. The residues involved include GLU 291, SER 101, and TRP 98; GLU 291, TYR 259, ASP 284, and SER 101; ASN 104, ALA 102, GLU 291, and SER 101, respectively. Other interactions between these ligands and the amino acid residues of 6GPS include hydrophobic and polar interactions.

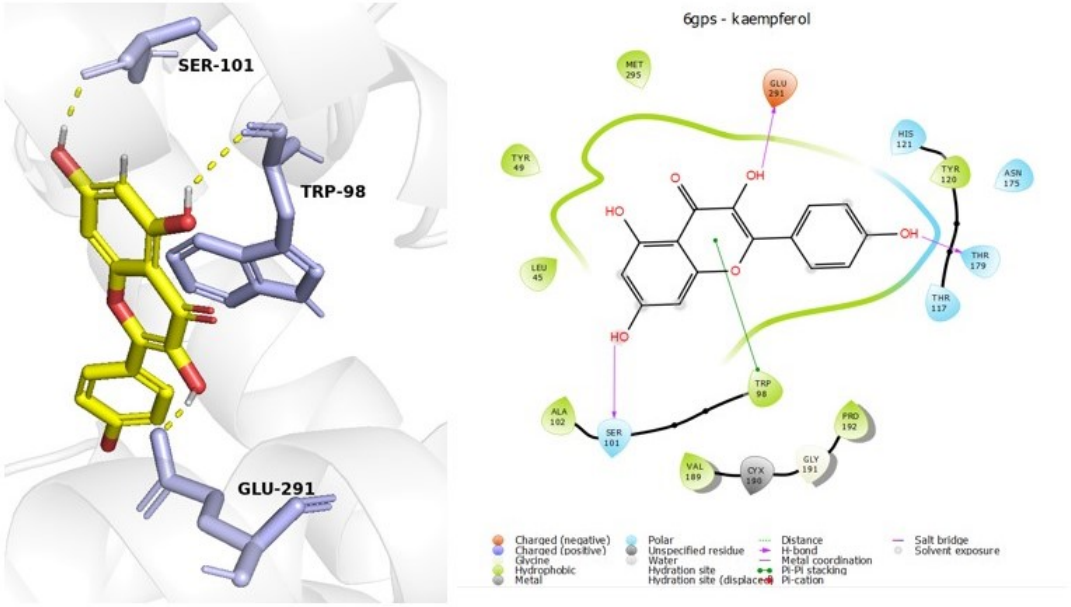

Figure 12: Molecular interaction of amino-acid residues of chemokine receptor 2 with Kaempferol. 3D left, 2D right.

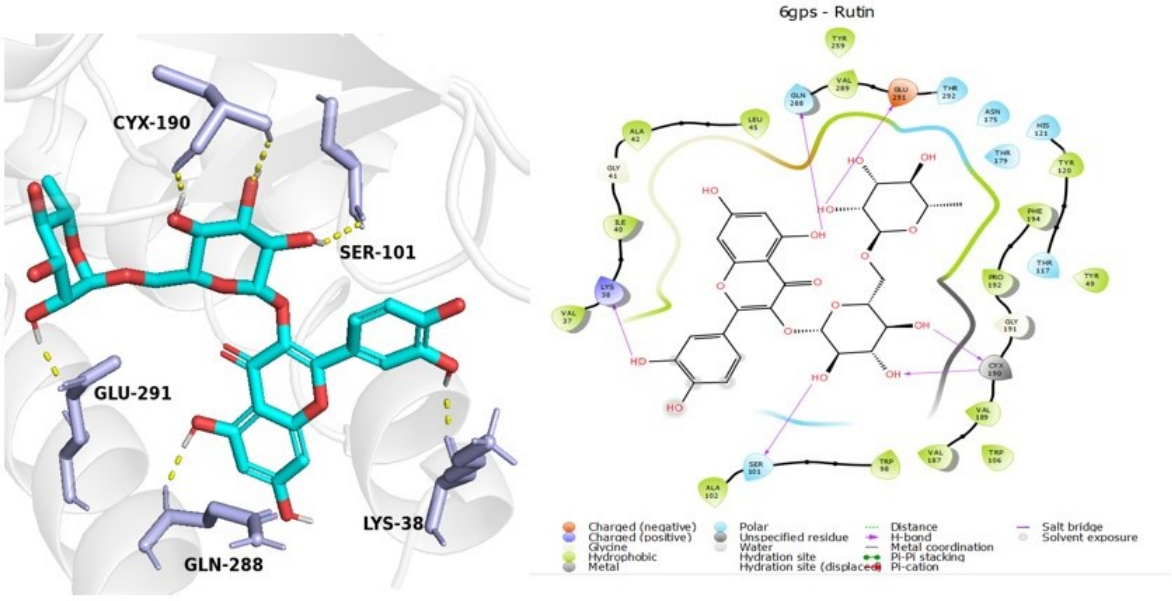

Figure 13: Molecular interaction of amino-acid residues of chemokine receptor 2 with Rutin. 3D left, 2D right.

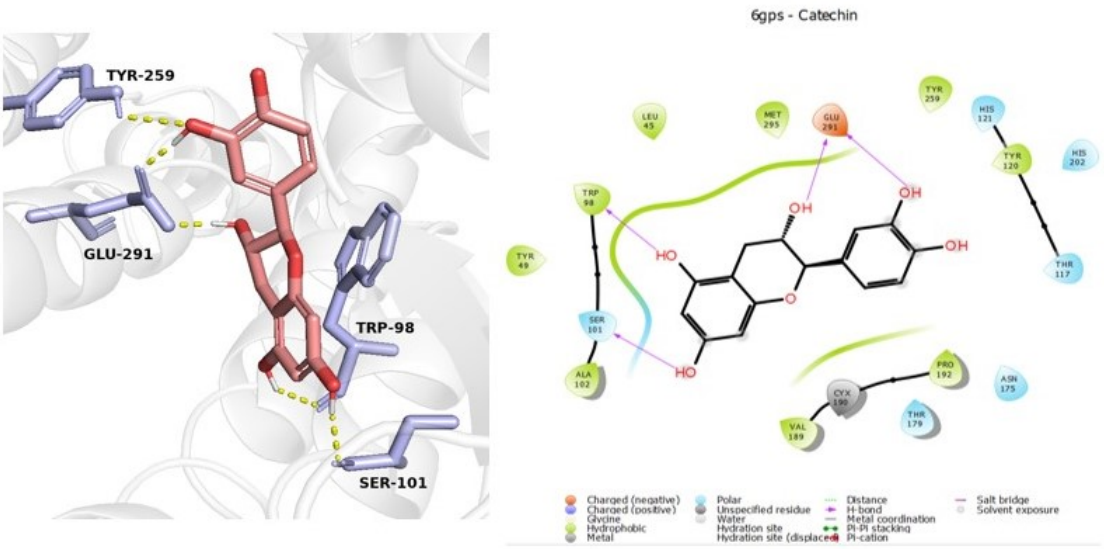

Figure 14: Molecular interaction of amino-acid residues of chemokine receptor 2 with Catechin. 3D left, 2D right.

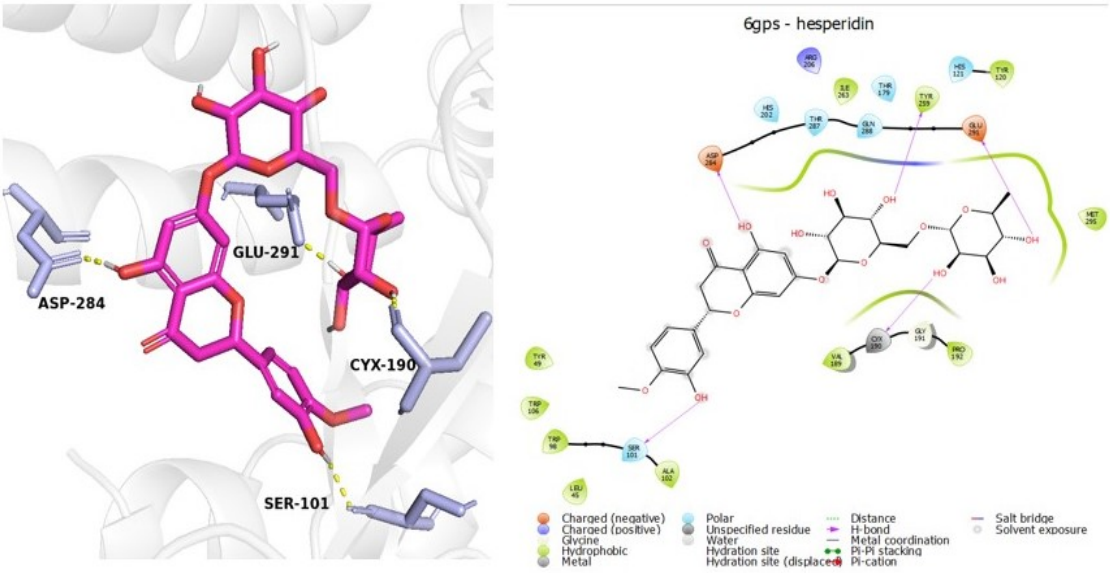

Figure 15: Molecular interaction of amino-acid residues of chemokine receptor 2 with Hesperidin. 3D left, 2D right.

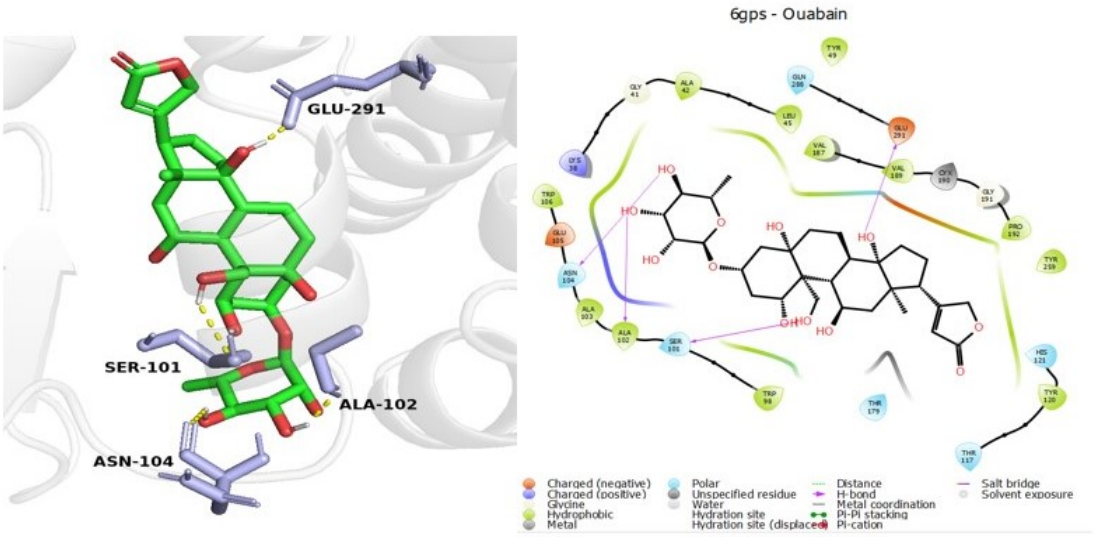

Figure 16: Molecular interaction of amino-acid residues of chemokine receptor 2 with Ouabain. 3D left, 2D right.

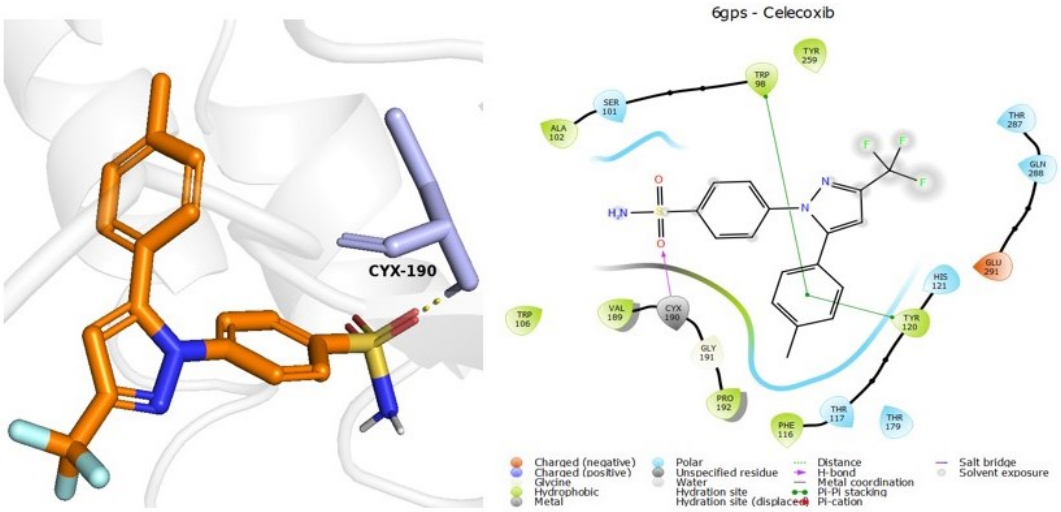

Figure 17: Molecular interaction of amino-acid residues of chemokine receptor 2 with the standard ligand (Celecoxib). 3D left, 2D right.

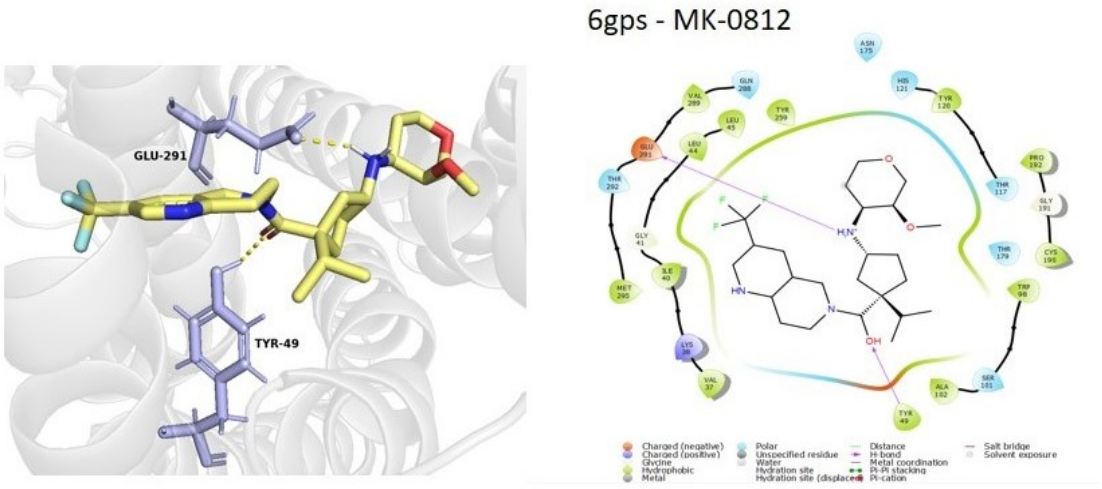

Figure 18: Molecular interaction of amino-acid residues of chemokine receptor 2 with the co-crystalised ligand (MK-0812). 3D left, 2D right

Table 2: Docking scores of the top 5 ranking compounds and the standard ligand against the target protein of cyclooxygenase-2

S/N	Name of compound	PubChem CID	Molecular formula	Molecular weight (g/mol)	Docking score (kcal/mol)
1	Rutin	5280805	$C_{27}H_{30}O_{16}$	610.5	-9.4
2	Hesperidin	10621	$C_{28}H_{34}O_{15}$	610.6	-7.9
3	Epicatechin	72276	$C_{15}H_{14}O_6$	290.27	-7.5
4	Phytate	890	$C_6H_{18}O_{24}P_6$	660.04	-7.5
5	Catechin	9064	$C_{15}H_{14}O_6$	290.27	-7.3
6	Standard drug (Celecoxib)	2662	$C_{17}H_{14}F_3N_3O_2S$	381.4	-6.4

Table 3: Docking scores of the top 5 ranking compounds and the standard ligand against the target protein of chemokine receptor type 2

S/N	Name of compound	PubChem CID	Molecular formula	Molecular weight (g/mol)	Docking score (kcal/mol)
1	Kaempferol	5280863	$C_{15}H_{10}O_6$	286.24	-7.9
2	Rutin	5280805	$C_{27}H_{30}O_{16}$	610.5	-7.7
3	Catechin	9064	$C_{15}H_{14}O_6$	290.27	-7.1
4	Hesperidin	10621	$C_{28}H_{34}O_{15}$	610.6	-6.9
5	Ouabain	439501	$C_{29}H_{44}O_{12}$	584.7	-6.9
6	Standard drug (Celecoxib)	2662	$C_{17}H_{14}F_3N_3O_2S$	381.4	-5.5

Table 4: Interactions of the top 5 compounds of *D.praehensilis* and the standard ligand against the target protein of cyclooxygenase-2

S/N	Ligand Name	PubChem ID	Type of Interaction				
			H-bonding	Hydrophobic	Polar	Pi-pi stacking	Pi-cation
1.	Rutin	5280805	ASN-144, SER-143, TRP-139, LYS-333, ARG-222	LEU-145, PHE-142, TRP-139, LEU-238, LEU-224	ASN-231, GLN-241, THR-237, GLN-330	-	-
2.	Hesperidin	10621	GLY-536, ARG-376, GLU-236	LEU-238, LEU-145, PHE-142	SER-143, ASN-144, GLN-374	PHE-142	-
3.	Epicatechin	72276	GLY-235, LYS-333, GLN-241, TRP-139, SER-143	LEU-145, LEU-224, TYR-234, LEU-238	ASN-231, ASN-144, THR-237	-	-
4.	Phytate	890	GLU-236, LYS-333, TRP-139, LEU-238, LEU-224	PHE-142, LEU-145, TRP-139	THR-237, ASN-231, SER-146, ASN-144	-	-
5.	Catechin	9064	GLY-235, GLN-241, GLU-140, LEU-224	LEU-238, TYR-234, LEU-145	ASN-231, SER-143, GLN-241, THR-237	-	-
6.	Celecoxib	2662	GLU-140	TRP-139, PHE-142, LEU-145,LEU 238	SER146, ASN 144, SER 143, GLN 241, THR 237		

Table 5: Interactions of the top 5 compounds of *D.praehensilis* and the standard ligand against the target protein of chemokine receptor 2

S/N	Ligand Name	PubChem ID	Type of Interaction				
			H-bonding	Hydrophobic	Polar	Pi-pi stacking	Pi-cation
1.	Kaempferol	5280863	SER-101, GLU-291, THR-179	TYR-120, ALA-102, PRO-192	HIS-121, ASN-175, THR-117	TRP-98	-
2.	Rutin	5280805	LYS-38, GLN-288, GLU-291, SER-101	PHE-194, PRO-192, VAL-189, VAL-37	THR-117, ASN-175, THR-292, HIS-121	-	-
3.	Catechin	9064	SER-101, GLU-291, TRP-98	TYR-120, MET-295, TYR-49	THR-179, ASN-175, HIS-121	-	-
4.	Hesperidin	10621	GLU-291, TYR-259, ASP-284, SER-101	PRO-192, VAL-189, TYR-120, TRP-106	HIS-202, THR-287, GLN-288, HIS-121	-	-
5.	Ouabain	439501	ASN-104, ALA-102, GLU-291, SER-101	TYR-120, TYR-259, VAL-189, ALA-103	HIS-121, THR-117, THR-179, GLN-288	-	-
6.	Celecoxib	2662	Unspecified residue at position190	TYR-259, PHE-116, PRO-192	HIS-121, THR-287, GLN-288	TRP-98, TYR-120	-

Pharmacokinetic and Toxicity Profile

Table 6 presents the predicted lipophilicity, water solubility, drug-likeness, and pharmacokinetic profiles of the compounds from *D. praehensilis*. The molecular weights of the selected compounds ranged from 286.24 to 660.04 g/mol, and Log S values ranged from -3.82 to 8.57, with all compounds classified as soluble. Log P ranged from -6.77 to 1.58. Three compounds, namely epicatechin, catechin, and kaempferol, did not violate the Lipinski rule of five (Ro5) and showed high GI absorption, with bioavailability scores of 0.55, while the remaining four had three violations each of Ro5, low GI absorption, and a bioavailability score of 0.17. All compounds showed unacceptable skin permeability, with high negative Log Kp values ranging from -17.63 to -6.7 cm/s. None of the compounds was predicted to cross the blood-brain barrier. Five of the compounds, namely rutin, hesperidin, epicatechin, phytic acid, and catechin, were predicted to be permeability glycoprotein (Pgp) substrates. None of the compounds was predicted to be an inhibitor of CYP2C19 or CYP2C9, while kaempferol was the only compound predicted to be an inhibitor of CYP1A2, CYP2D6, and CYP3A4.

Table 7 shows the toxicity profile of the compounds. Rutin, hesperidin, epicatechin, phytic acid, catechin, kaempferol, and ouabainhaveLD50 values of 5000, 12000, 10000, 1500, 10000, 3919, and 5 mg/kg, respectively, and belong to classes 5, 6,6, 4, 6, 5, and 1, respectively. For organ toxicity prediction, all the compounds were predicted to show nephrotoxicity and respiratory toxicity,while Ouabain was also predicted to be cardiotoxic. None was hepatotoxic nor neurotoxic. For the toxicity endpoint prediction, all the compounds were predicted to show nutritional toxicity, while only ouabain was predicted to be cytotoxic and immunotoxic.

Table 6: Pharmacokinetics prediction and drug likeness of some compounds from *Dioscorea praehensilis*

	C1	C2	C3	C4	C5	C6	C7
Molecular weight (g/mol)	610.52	610.56	290.27	660.04	290.27	286.24	584.65
Silicos IT Log Sw	-0.29	-0.58	-2.14	8.57	-2.14	-3.82	0.33
Silicos IT class	Soluble	Soluble	Soluble	Soluble	Soluble	Soluble	Soluble
Consensus Log P	-1.51	-1.06	0.85	-6.77	0.83	1.58	-0.47
Lipinski violations	3	3	0	3	0	0	3
TPSA	269.43	234.29	110.38	457.42	110.38	111.13	206.66
Bioavailability score	0.17	0.17	0.55	0.11	0.55	0.55	0.17
Log Kp (cm/s)	-10.26	-10.12	-7.82	-17.63	-7.82	-6.7	-11.07
GI Absorption	Low	Low	High	Low	High	High	Low
BBB permeant	No	No	No	No	No	No	No
Pgp substrate	Yes	Yes	Yes	Yes	Yes	No	No
CYP1A2 inhibitor	No	No	No	No	No	Yes	No
PAINS alert	1	0	1	0	1	0	0
CYP1A2 inhibitor	No	No	No	No	No	Yes	No
CYP2C19 inhibitor	No	No	No	No	No	No	No
CYP2C9 inhibitor	No	No	No	No	No	No	No
CYP 2D6 inhibitor	No	No	No	No	No	Yes	No
CYP3A4 inhibitor	No	No	No	No	No	Yes	No

BBB. Blood-brain barrier,GI. Gastrointestinal, TPSA. Total polar surface area, C1. Rutin, C2. Hesperidin, C3. Epicatechin, C4. Phytic acid, C5.Catechin, C6. Kaempferol, C7. Ouabain

Table 7: Toxicity profile of compounds from *Dioscorea praehensilis*

Target	Compound						
	C1	C2	C3	C4	C5	C6	C7
Predicted LD_{50} (mg/kg)	5000	12000	10000	1500	10000	3919	5
Predicted Toxicity Class	5	6	6	4	6	5	1
Hepatotoxicity	No	No	No	No	No	No	No
Neurotoxicity	No	No	No	No	No	No	No
Nephrotoxicity	Yes	Yes	Yes	Yes	Yes	Yes	Yes
Respiratory Toxicity	Yes	Yes	Yes	Yes	Yes	Yes	Yes
Cardiotoxicity	No	No	No	No	No	No	Yes
Carcinogenicity	No	No	No	No	No	No	No
Immunotoxicity	Yes	Yes	No	No	No	No	Yes
Mutagenicity	No	No	No	No	No	No	No
Cytotoxicity	No	No	No	No	No	No	Yes
Nutritional Toxicity	Yes	Yes	Yes	Yes	Yes	Yes	Yes

LD= Lethal dose, C1. Rutin, C2. Hesperidin, C3. Epicatechin, C4. Phytic acid, C5. Catechin, C6. Kaempferol, C7. Ouabain

Discussion

In the present study, we evaluated the potential antinociceptive and anti-inflammatory effects of *D.praehensilis* methanol extract *in-vivo*, using different pharmacological approaches, including the tail-flick test, hot-plate test, formalin-induced paw oedema, and *in-silico,* using two protein targets. Our results showed that *D. praehensilis* exhibited statistically significant antinociceptive and anti-inflammatory effects in extract-treated animals compared with the vehicle-treated control. Furthermore, using *in silico* techniques, we have demonstrated that bioactive compounds present in *D. praehensilis* can inhibit the cyclooxygenase-2 enzyme and the chemokine receptor 2 target protein. Additionally, we have shown that these compounds have good pharmacokinetic properties and drug likeness with an acceptable safety profile.

The hot plate method is appropriate for assessing central nociceptive activity. (Sharma *et al*., 2019) while the tail-flick test measures the latencies of spinal nociceptive responses to a thermal stimulus (Cavendish *et al*., 2015). The two tests are simple and commonly used to investigate analgesic efficacy, and are more sensitive to opioid analgesics (Karna *et al*., 2019). An increase in reaction time is typically considered a key factor in assessing the central antinociceptive activity in these models. (Rujjanawate, *et al*., 2003).The significant ($p<0.01$ and $p<0.05$) increase in latency time of rats at 40- and 60 min post-administration, respectively, at different doses in the tail flick model, indicates that *D. prehensilis* has a central antinociceptive activity. This may be related to the inhibition of agents that activate the release of the endogenous peptide by periaqueductal gray matter, which is carried to the spinal cord to inhibit pain muscle transmission within the dorsal horn (Shilo and Pascoe, 2014). A rather more profound central antinociceptive activity was depicted in the hot plate model that shows a significant ($p<0.01$) increase in latency time right from 20 min post administration, which was maintained throughout the study period with a significance of $p<0.0001$ for 200 mg/kg extract at 60 min post administration. This may suggest modulation of the medullary or central pain mechanism with a direct inhibitory activity on

nerve endings or transmission pathways (Bomba *et al*., 2015).

The model used to evaluate the anti-inflammatory effect in this study was the formalin paw oedema test. Subplantar injection of formalin into the rat paw causes an acute and progressive increase in volume in the injected paw. This oedema is a hallmark of acute inflammation, driven by increased vascular permeability that results in the leakage of transvascular fluid rich in high-molecular-weight proteins from the intravascular to the interstitial compartment (Aller *et al*., 2007). The inflammation produced in this model consists of two phases. The first phase, which occurs 1 or 1.5 hours after formalin administration, produces oedema that is primarily mediated by pro-inflammatory mediators, such as histamine, bradykinin, and serotonin (Zhu *et al*., 2011). The second phase (2-5 hours) is characterised by a further increase in oedema formation that lasts up to 5 hours, with a maximum peak at 3 hours, and is normally maintained by other mediators, such as cytokines, namely Interleukin 1 beta (IL-1β) and Tumour Necrosis Factor-alpha (TNF-α), prostaglandins, and nitric oxide (Khan *et al*., 2009). The results of this study showed that *D.praehensilis* methanol extract treatment inhibited formalin-induced inflammation. Treatment at a dose of 200 mg/kg produced a significant reduction in paw oedema in the 3rd and 4th hours. This effect may be due to inhibition of the inflammatory cascade and of prostaglandin synthesis.

To further validate the potential antinociceptive and anti-inflammatory properties of *D. praehensilis*, computer–aided drug discovery (CADD) was employed to investigate the binding affinities of its bioactive compounds for cyclooxygenase-2 and chemokine receptor-2 proteins. CADD and virtual screening have transformed the drug discovery process by helping identify potential drug candidates while reducing costs and time (Alhashemi *et al*., 2025). Molecular docking techniques are an important tool for identifying compounds with the lowest binding energy, indicating strong binding affinity for a given receptor (Dauda *et al*., 2026).

Generally, a lower docking score (i.e., greater negativity) indicates a rational and stable interaction between the ligand and the protein (Feng *et al*., 2020). Notably, our results indicate that some of the test compounds exhibit stronger binding affinity for COX-2 and chemokine receptor-2 than a known COX-2 inhibitor (celecoxib), suggesting that *D. praehensilis* contains compounds that could interact well with these receptors.

Although several receptors are implicated in nociception and inflammation (Alhashemi *et al*., 2025), the cyclooxygenase enzyme system is the major pathway, catalysing the conversion of arachidonic acid into prostaglandins (Norregaard *et al*., 2015). Although the enzyme exists in two isoforms (COX-1 and COX-2), the COX-2 isoform is highly induced by inflammation and tissue injury (Norregaard *et al*., 2015). Inhibition of COX-2 is a good target for nociception and inflammation, and most non-steroidal anti-inflammatory drugs and selective COX-2 inhibitors exert their pharmacological action through COX-2 inhibition. Notably, all identified compounds in *D. praehensilis* showed favourable interactions with COX-2, with only two having docking scores below -5.4 kcal/mol. Furthermore, these compounds displayed higher affinity for COX-2, with the top-ranking compound achieving a docking score of -9.0 kcal/mol, higher than that of the top-ranking compound of 6GPS (7.9 kcal/mol). This further establishes the key role COX-2 plays as a major regulator of nociception and inflammation. Furthermore, the docking scores obtained for the test compounds were higher than those of the known COX-2 inhibitor celecoxib. Hence, we have shown that the bioactive compounds in *D. praehensilis* can interact effectively with COX-2.

In our study, the predominant interactions observed between the top-ranking compounds and the amino acid residues of COX-2 were hydrogen bonding, hydrophobic, and polar interactions. However, Hong *et al*. (2024), in a similar study on COX-2-inhibiting peptides present in walnuts, reported predominantly hydrogen bonding and hydrophobic interactions. Although 5COX lacked a co-crystallised compound, the top-ranking

compounds showed interactions similar to those observed for the standard ligand, celecoxib, with COX-2. These common residues include TRP 139, LEU 145, PHE 142, LEU 238, SER 146, ASN 144, GLN 241, and THR 237. Studies have demonstrated that protein sequences containing cyclic or aromatic amino acids could have great potential for designing structures that can serve as COX-2 inhibitors (Ahmaditaba *et al*., 2017), and that these sequences can exhibit anti-inflammatory (Nankar and Pande, 2014) and antioxidant activity (Suttisuwan *et al*., 2019). Furthermore, previous evidence has demonstrated that the active site of COX-2 predominantly contains hydrophobic amino acid residues (Rouzer and Marnett, 2020), which could enhance the binding of hydrophobic peptides to COX-2 (Gupta *et al*., 2017).

The chemokine receptor 2 (CCR2) is the main receptor for monocyte chemoattractant protein-1 and plays an important role in the immune system, mediating monocyte and macrophage recruitment to inflammatory sites (Park *et al*., 2022), and the absence of CCR2 reduces inflammation (Boring *et al*., 1997; Kuziel *et al*., 1997). Two isoforms of CCR2, namely CCR2A and CCR2B, have been identified. These isoforms are produced from the same gene, and both promote inflammation. While CCR2B is a major player in acute inflammation, mediating the trafficking of inflammatory monocytes from the bone marrow to peripheral tissues, CCR2A is often associated with chronic inflammatory conditions, as it contributes to sustained, long-term inflammation, tissue remodelling, and cell proliferation (Park *et al*., 2022).

As observed with 5COX, the sample compounds interacted with amino acid residues in 6GPS that are similar to those of the standard ligand (celexocib). These residues include TYR 259, TYR 120, GLN 288, THR 287, and HIS 121. Furthermore, some amino acid residues involved in the interactions of the co-crystallised compound in 6GPS (MK-0812) were also involved in the interactions of the tested compounds. This implies that the sample compounds also interact with amino acid residues at the protein's active site. Additionally, peptides containing hydrophobic amino acids at the N-terminus exhibit greater biological activity (Acquah *et al*., 2018). The results of our study showed that the N-terminal amino acid residues involved in interactions with 5COX and 6GPS were mainly hydrophobic, including TRP, LEU, VAL, and GLY.

In silico ADMET analysis is an important tool for predicting drug absorption, distribution, metabolism, and excretion in the organism, and for assessing toxicological effects and the safety profile of drug candidates (Ugwah-Oguejiofor *et al*., 2025). The aim is to reduce pharmacokinetic and toxicity-related failures in the drug discovery process as drug candidates enter the clinical trial phase (Shah *et al*., 2019). Consequently, the pharmacokinetic properties, drug-likeness, and toxicological profile of the seven top-ranking compounds in this study were evaluated. Lipinski's Rule of 5, commonly known as the rule of five, is used to evaluate the drug-likeness of a compound and its suitability as an oral preparation. It predicts whether a biologically or pharmacologically active compound possesses physical and chemical properties that will make it orally bioavailable. Generally, a molecule is considered suitable if it does not violate more than one of the Ro5, which include: molecular weight less than 500 g/mol, octanol-water partition coefficient (Log P) less than 5, hydrogen bond donors less than 5, and hydrogen bond acceptors less than 10. In our study, three of the seven compounds, namely epicatechin, catechin, and kaemferol, did not violate any of the Ro5. These compounds had consensus Log P values ranging from 0 to 5, indicating lipophilicity that favours optimal absorption across biological membranes. The TPSA results for these compounds, which fall within the acceptable range of ≤140 (Shaikh *et al*., 2022), further confirm their optimal permeability. Additionally, these compounds had a bioavailability score of 0.55, indicating moderate to good oral bioavailability and a strong likelihood of systemic absorption (Knoll *et al*., 2022).

The remaining four compounds, namely rutin, hesperidin, phytic acid, and ouabain, violated some of the Ro5. They had molecular weights greater than 500 g/mol, suggesting low gastrointestinal absorption and impaired distribution to target sites of action (Salifu *et al*., 2023). Furthermore, the number of hydrogen bond donors and acceptors exceeded the Ro5 limits, indicating that they violated three of Lipinski's rules. Hence, they may not be suitable for oral administration. Their negative consensus Log P scores indicate that they are highly hydrophilic and may exhibit poor permeability across lipid-rich biological membranes, making them less likely to be absorbed by passive diffusion and potentially requiring different formulation strategies, such as active transport. The significantly higher TPSA scores of these compounds further demonstrate their inability to permeate biological membranes (Samuel *et al*., 2021). All tested compounds were predicted to be unlikely to penetrate the blood-brain barrier. This indicates a low probability of causing neurotoxicity. This may be beneficial, as some currently available NSAIDs have been associated with neurotoxic effects such as aseptic meningitis, seizures, dizziness, recurrent falls, encephalopathy, nystagmus, and disorientation (Morgan and Clark, 1998; Auriel *et al*., 2014). The cytochrome P450 (CYP) enzyme system plays important roles in the biotransformation of drugs and xenobiotics. It is involved in phase 1 metabolic reactions that introduce or expose polar functional groups on lipophilic drugs and xenobiotics, facilitating excretion or preparing them for phase 2 conjugation reactions (Gilani and Cassagnol, 2012). The majority of the tested compounds were predicted not to inhibit any of the CYP enzymes. This will minimise the possibility of drug-drug interactions that can lead to toxicity due to drug accumulation as a consequence of reduced metabolism of co-administered agents. Kaemferol, on the other hand, was predicted to inhibit CYP1A2, CYP2D6 and CYP3A4, showing potential interactions with co-administered agents.

Based on the predicted toxicity profile, all but one of the tested compounds belong to toxicity classes 4-6, with LD50 values ranging from 1500 to 12,000 mg/kg, except for ouabain, which belongs to toxicity class 1 with an LD_{50} of 5 mg/kg. Hence, the majority of the compounds can be administered within this permissible dosage without acute toxicity. Evaluation of the toxicity endpoints of the tested compounds revealed that all had the potential to cause nephrotoxicity, respiratory toxicity, and nutritional toxicity, with additional immunotoxicity with rutin and hesperidin, and cytotoxicity with ouabain. Structural modification of these compounds that retains or enhances efficacy while minimising these toxic effects would need to be considered.

A preliminary phytochemical analysis of the methanol extract of *D. praehensilis* revealed the presence of secondary metabolites, including saponins, tannins, flavonoids, steroids, and alkaloids (Adebisi *et al*., 2018b). A variety of compounds belonging to this class of secondary metabolites have been identified in the HPLC analysis presented in this study, some of which have been reported to have anti-inflammatory and antinociceptive effects in the literature. Mohammed *et al*. (2014) reported that saponins isolated from approximately 50 plants have demonstrated anti-inflammatory activity in several experimental models of inflammation in rats and mice. Phenolic compounds, such as flavonoids and tannins, have also been reported to exert anti-inflammatory effects by inhibiting pro-inflammatory enzymes, including cyclooxygenase and lipoxygenase (Tjølsen, 1992). Some alkaloids, such as isoquinolines, indoles, and diterpenes, are known to exhibit strong anti-inflammatory activity (Fawole *et al*., 2009), while major classes of bioactive steroids have also been reported to possess anti-inflammatory effects (Vassallo *et al*., 2013; Hieu *et al*., 2024; Dembitsky and Terent'ev, 2026).

This study has some limitations. Firstly, the tail-flick and hot-plate models of nociception are sensitive to motor impairment. In addition, these tests primarily evaluate acute, transient stimulus-evoked pain rather than chronic or neuropathic pain (Deuis *et al*., 2017). Secondly, though the

formalin induced paw oedema is biphasic, modeling both neurogenic and inflammatory pain respectively and favoured to study pain and early inflammation, formalin is a potent tissue irritant which may cause significant distress to the animal resulting in high level of paw licking behavior and swelling that could require high doses of test substances to show anti-inflammatory activity (Patil *et al*., 2019). In the *in silico* analysis, while the tested compounds demonstrated good binding affinities, limitations in GI absorption, low bioavailability scores for some compounds, and the inability to cross the BBB may hinder their effectiveness as drug candidates. Furthermore, some predicted toxicities, including nephrotoxicity, respiratory toxicity, and nutritional toxicity, may pose safety concerns and require evaluation in biological models.

Conclusion

In conclusion, the methanol extract of *D. praehensilis* rhizomes exhibited significant antinociceptive and anti-inflammatory activity in animal models. In addition, using molecular docking, we have shown that some bioactive compounds from this plant exhibit strong binding affinities for cyclooxygenase-2 and chemokine receptor-2, with acceptable drug-likeness and safety profiles. The findings of the study validate the use of *D. praehesilis* rhizomes as a folk medicine for the treatment of inflammatory conditions and provide a basis for further studies exploring this plant as a source of novel therapeutic agents for the treatment of nociception and inflammation.

Conflict of interest

The authors declared no conflict of interest

References

Acquah, C., Di Stefano, E., Udenigwe, C. C. 2018. Role of hydrophobicity in food peptide functionality and bioactivity. Journal of Food Bioactives, 4: 88-98.

Adebisi, I. M., Ojoh, H. I., Suleiman, A., Ugwah-Oguejiofor, C. J., & Salihu, A. 2025.Wound-healing activity of *Dioscorea praehensilis* is associated with upregulation of VEGF gene expression in a rat model. FUDMA journal of sciences, 9(9): 250-256. https://doi.org/10.33003/fjs-2025-0909-3732

Adebisi, I.M., Bello, S.O., Shehu, C.E., Abdullahi, M.I., UgwahOguejiofor, C.J., Ndodo, N., Umar, M. 2018[a]. *Dioscorea prehensilis* ameliorates the features of preeclampsia in the Nω-nitro-L-arginine methyl ester (L-NAME) preeclamptic model. *Tropical Journal of Natural Product Research*, 2(9):422-428.

Adebisi, I.M., Bello, S.O., Shehu, C.E., Musa, A., Halilu, M.E., Sulaiman, A. 2018[b]. Quantitative Phytochemicals and Inhibitory Effect of Methanol Extract of *Dioscorea prehensilis* on Platelet Aggregation in vitro. Nigerian Journal of Pharmaceutical and Biomedical Research 3(1):41-45.

Ahmaditaba, M. A., Shahosseini, S., Daraei, B., Zarghi, A., & Houshdar Tehrani, M. H. 2017. Design, synthesis, and biological evaluation of new peptide analogues as selective COX-2 inhibitors. Archiv der Pharmazie, 350(10): 1700158.

Alhashemi, S. H., Zare, F., Sadeghian, S., Poustforoosh, A., & Dehshahri, A. 2025. Identification of potential natural analgesic compounds through molecular docking-virtual screening, molecular dynamics simulation, MM/GBSA, DFT, and ADMET computations. Scientific Reports, 15: 39995. https://doi.org/10.1038/s41598-025-23655-y

Alhassen, L., Dabbous, T., Ha, A., Dang, L. H. L., &Civelli, O. 2021. The Analgesic Properties of Corydalis yanhusuo. Molecules, 26(24): 7498.

Aller, M.A., Arias, J.L., Arias, J.I., Sanchez-Patan, F. and Arias, J. 2007. The inflammatory response recapitulates phylogeny through trophic mechanisms to

the injured tissue. Medical hypotheses, 68(1): 202-209.

Apel, A. K., Cheng, R. K. Y., Tautermann, C. S., Brauchle, M., Huang, C. Y., Pautsch, A., Hennig, M., Nar, H., &Schnapp, G. (2019). Crystal Structure of CC Chemokine Receptor 2A in Complex with an Orthosteric Antagonist Provides Insights for the Design of Selective Antagonists. Structure (London, England: 1993), 27(3), 427–438.e5. https://doi.org/10.1016/j.str.2018.10.027.

Auriel, E., Regev, K., &Korczyn, A. D. 2014. Nonsteroidal anti-inflammatory drugs exposure and the central nervous system. Handbook of clinical neurology, 119: 577-584.

Banerjee, P., Kemmler, E., Dunkel, M., & Preissner, R. 2024. ProTox 3.0: a webserver for the prediction of toxicity of chemicals. Nucleic Acids Research, 52(W1), W513-W520.

Bomba, F.D.T., Wandji, B.A., Piegang, B.N., Awouafack, M.D., Sriram, D., Yogeeswari, P., Kamanyi, A. and Nguelefack, T.B. 2015. Antinociceptive properties of the aqueous and methanol extracts of the stem bark of *Petersianthus macrocarpus* (P. Beauv.) Liben (Lecythidaceae) in mice. J. Ethnopharmacol. 174: 66-73.

Boring, L., Gosling, J., Chensue, S. W., Kunkel, S. L., Farese, R. V., Broxmeyer, H. E., & Charo, I. F. 1997. Impaired monocyte migration and reduced type 1 (Th1) cytokine responses in CC chemokine receptor 2 knockout mice. *J Clin Invest. 100(10): 2552–2561. doi: 10.1172/JCI119798.*

Cavendish, R.L., de Souza Santos, J., Neto, R.B., Paixão, A.O., Oliveira, J.V., de Araujo, E.D., e Silva, A.A.B., Thomazzi, S.M., Cardoso, J.C. and Gomes, M.Z. 2015. Antinociceptive and anti-inflammatory effects of Brazilian red propolis extract and formononetin in rodents. J. Ethnopharmacol. 173:127-133.

Chu, H.X., Arumugam, T.V., Gelderblom, M., Magnus, T., Drummond, G.R. and Sobey, C.G. 2014. Role of CCR2 in inflammatory conditions of the central nervous system. Journal of Cerebral Blood Flow & Metabolism, 34(9): 1425-1429.

Daina, A., Michielin, O. and Zoete, V. 2017. Swiss ADME: a free web tool to evaluate pharmacokinetics, drug-likeness and medicinal chemistry friendliness of small molecules. Scientific reports, 7(1): 42717.

D'Amour, F.E. and Smith, D.L. 1941. A method for determining loss of pain sensation. J PharmacolExpTher, 72(1): 74- 79.

Dauda, G., Olorukooba, A.B., Adebisi, I.M., Ogundele, O.I., Jibril, M.M., Igharo, A.K., Sani, J., Iorjiim, W.M., Abiola, O.M., Adegboyega, A.E. and Johnson, T.O., 2026. Molecular docking and dynamics identify novel high-affinity plasmepsin II inhibitors from neem phytochemicals for antimalarial drug development. Discover Chemistry. *3*(1): 6.

Dembitsky, V. M., &Terent'ev, A. O. 2026. Steroidal Compounds at the Crossroads of Inflammation and Cancer: Implications for Drug Discovery and Therapy. Biomedicines, 14(1): 214.

Desai, S.J., Prickril, B. and Rasooly, A., 2018. Mechanisms of phytonutrient modulation of cyclooxygenase-2 (COX-2) and inflammation related to cancer. Nutrition and cancer, 70(3): 350-375.

Deuis, J. R., Dvorakova, L. S., & Vetter, I. 2017. Methods used to evaluate pain behaviors in rodentsFrontMolNeurosci 10: 284

Eddy, N.B. and Leimbach, D. 1953. Synthetic analgesics. II. Dithienylbutenyl-and dithienylbutylamines. Journal of Pharmacology and Experimental Therapeutics, 107(3): 385-393.

Fawole, O.A., Ndhlala, A.R., Amoo, S.O., Finnie, J.F. and Van Staden, J. 2009. Anti-inflammatory and phytochemical properties of twelve medicinal plants used for treating gastrointestinal ailments in South Africa. J. Ethnopharmacol. 123(2): 237-243.

Feng, J., Ma, Y. L., Sun, P., Thakur, K., Wang, S., Zhang, J. G., & Wei, Z. J. 2021. Purification and characterisation of α-glucosidase inhibitory peptides from defatted camellia seed cake .Int. J. Food Sci. Technol. 56 (1): 138-147. https://doi.org/10.1111/ijfs.14613.

Gilani, B., and Cassagnol, M. 2021. "Biochemistry, Cytochrome P450," in StatPearls. Treasure Island (FL): StatPearls Publishing Copyright © 2021 (StatPearls Publishing LLC.). Accessed on 11th February, 2026.

Gupta, S., Sharma, A. K., Shastri, V., Madhu, M. K., & Sharma, V. K. 2017. Prediction of anti-inflammatory proteins/peptides: an insilico approach. Journal of translational medicine, 15(1): 7. https:// doi.org/10.1186/s12967-016-1103-6

Han, H., Ro, D. H., Han, H. S., & Won, S. 2025. Overall compilation of adverse effects of non-steroidal anti-inflammatory drugs: a hypothesis-free systematic investigation using a nationwide cohort study. Front Pharmacol. 16: 1539328. doi: 10.3389/fphar.2025.1539328.

Hieu, N.V., Vinh, L.B., Phong, N.V., Cong, P.V., Dat, N.T., Dan, N.V., Duc, N.V., Tao, H.M., Tam, L.T., Anh, L.T. and Cuong, N.C., 2024. Two New Steroidal Saponins with Potential Anti-Inflammatory Effects from the Aerial Parts of GnetumformosumMarkgr. Plants. 13(15): 2100.

Hong, Z., Xie, J., Tao, L., Dai, J.J., Li, T., Zhang, L., Bai, Y., Hu, X., Chen, J., Sheng, J. and Tian, Y., 2024. Exploration of cyclooxygenase-2 inhibitory peptides from walnut dreg proteins based on in silico and in vitro analysis. Food Science and Human Wellness. 13(3): 1636-1644.
https://doi.org/10.3389/fddsv.2023.1087008

Ilesanmi, O. S., Adedugbe, O. F., and Adewale, I. O. 2021. Potentials of purified tyrosinase from yam (Dioscorea spp) as a biocatalyst in the synthesis of cross-linked protein networks. Heliyon, 7(8): e07831.

Karna, S.R., Kongara, K., Singh, P.M., Chambers, P. and Lopez-Villalobos, N. 2019. Evaluation ofanesthesiainteraction between morphine, dexmedetomidine and maropitant using hot-plate and tail-flick tests in rats. Veterinary anaesthesia and analgesia, 46(4): 476-482.

Katzung, B.G. 2017. Basic and clinical pharmacology 14th edition. McGraw Hill Professional.

Khan, I., Nisar, M., Ebad, F., Nadeem, S., Saeed, M., Khan, H., Khuda, F., Karim, N. and Ahmad, Z. 2009. Anti-inflammatory activities of Sieboldogenin from Smilax china Linn.: experimental and computational studies. J. Ethnopharmacol. 121(1): 175-177.

Knoll, K. E., van der Walt, M. M., and Loots, D. T. 2022. In silico drug discovery strategies identified ADMET properties of decoquinate RMB041 and its potential drug targets against Mycobacterium tuberculosis. Microbiology Spectrum, 10(2): e02315-21.

Kumar, K.H. and Elavarasi, P. 2016. Definition of pain and classification of pain disorders. Journal of Advanced Clinical and Research Insights, 3(3): 87-90.

Kurumbail, R. G., Stevens, A. M., Gierse, J. K., McDonald, J. J., Stegeman, R. A., Pak, J. Y., Gildehaus, D., Miyashiro, J. M., Penning, T. D., Seibert, K., Isakson, P. C., & Stallings, W. C. (1996). Structural basis for selective inhibition of cyclooxygenase-2 by anti-inflammatory agents. Nature, 384(6610), 644–648. https://doi.org/10.1038/384644a0.

Kuziel, W. A., Morgan, S. J., Dawson, T. C., Griffin, S., Smithies, O., Ley, K., & Maeda, N. 1997. Severe reduction in leukocyte adhesion and monocyte extravasation in mice deficient in CC chemokine receptor 2. *ProcNatlAcadSci U S A. 94(22):12053–12058. doi: 10.1073/pnas.94.22.12053.*

Mohammed, M.S., Osman, W.J., Garelnabi, E.A., Osman, Z., Osman, B., Khalid, H.S. and Mohamed, M.A. 2014. Secondary metabolites as anti-inflammatory agents. J Phytopharmacol, 3(4): 275-85.

Morgan, A. and Clark, D. 1998. CNS adverse effects of nonsteroidal anti-inflammatory drugs: therapeutic implications. CNS drugs. 9(4): 281-290.

Nankar, S.A. and Pande, A.H., 2014. Properties of apolipoprotein E derived peptide modulate their lipid-binding capacity and influence their anti-inflammatory function. *Biochimicaet BiophysicaActa (BBA)*-Molecular and Cell Biology of Lipids, 1841(4): 620-629. https://doi.org/10.1016/j.bbalip.2014.01.006.

Nørregaard, R., Kwon, H., & Frøkiær, J. 2015. Physiology and pathophysiology of cyclooxygenase-2 and prostaglandin E2 in the kidney. Kidney Research and Clinical Practice, 34(4): 194. https://doi.org/10.1016/j.krcp.2015.10.004

Paradee, N., Koonyosying, P., Kusirisin, W., Janthip, R., Kanjanapothi, D., Pattanapanyasat, K., & Srichairatanakool, S. 2021. Analgesic, anti-inflammatory and anti-ulcer properties of Thai Perilla frutescence fruit oil in animals. Bioscience Reports, 41(1): BSR20203166.

Park, H.K., Na, Y.H., Nguyen, H.T., Nguyen, L.P., Hurh, S., Seong, J.Y., Lee, C.S., Ham, B.J. and Hwang, J.I., 2022. Analysis of CCR2 splice variant expression patterns and functional properties. Cell & Bioscience, 12(1): 59.

Patil, K. R., Mahajan, U. B., Unger, B. S., Goyal, S. N., Belemkar, S., Surana, S. J., Ojha S., and Patil, C. R. 2019. Animal models of inflammation for screening of anti-inflammatory drugs: implications for the discovery and development of phytopharmaceuticals. International journal of molecular sciences, 20(18): 4367.

Rouzer, C. A. and Marnett, L. J. 2020. Structural and chemical biology of the interaction of cyclooxygenase with substrates and non-steroidal anti-inflammatory drugs. Chemical Reviews, 120(15): 7592-7641.

Rujjanawate, C., Kanjanapothi, D. and Panthong, A. 2003. Pharmacological effect and toxicity of alkaloids from Gelsemium elegans Benth. J. Ethnopharmacol. 89(1): 91-95.

Salifu, E. Y., Abugri, J., Rashid, I. A., Osei, F., and Ayariga, J. A. 2023. In silico identification of potential inhibitors of acyl carrier protein reductase and acetyl CoA carboxylase of *Plasmodium falciparum* in antimalarial therapy. Front Drug. Discov. 3: 1087008.

Samuel, B. B., Oluyemi, W. M., Johnson, T. O., and Adegboyega, A. E. 2021. High-Throughput Virtual Screening with Molecular Docking, Pharmacophore Modelling and ADME Prediction to Discover Potential Inhibitors of Plasmodium falciparum Lactate Dehydrogenase (PfLDH) from Compounds of Combretaceae Family: doi. org/10.26538/tjnpr/v5i9. 22. Tropical Journal of Natural Product Research (TJNPR), 5(9): 1665-1672. https://doi.org/10.26538/tjnpr/v5i9.22

Schrödinger (2020). Maestro release 2020-3. Schrödinger. LLC, New York, NY, USA, 2020.

Shah, A. P., Parmar, G. R., Sailor, G. U., & Seth, A. K. 2019. Antimalarial phytochemicals identification from Euphorbia hirta against plasmepsin protease: an in silico approach. Folia medica, 61(4): 584-593.https://doi.org/10.3897/folmed.61.e47965

Shaikh, M. S., Islam, F., Gargote, P. P., Gaikwad, R. R., Dhupe, K. C., Khan, S. L., ... & Emran, T. B. 2022. Potential EphA2 receptor blockers involved in cerebral malaria from *Taraxacum officinale, Tinospora cordifolia, Rosmarinus officinalis* and *Ocimum basilicum*: a computational approach. Pathogens, 11(11): 1296.

https://doi.org/10.3390/pathogens 11111296

Sharma, S., Khare, Sacid-inducedK., Joshi, A. and Jain, A. 2019. Analgesic activity of poly herbal formulation in experimental rats by acetic acid induced writhing test model and Hot plate model. Journal of Drug Delivery and Therapeutics, 9(2-s): 276-280.

Shilo Y., Pascoe P.J. In: Pain Management in Veterinary Practice. Egger C.M., Love T., Doherty T., editors. John Wiley & Sons, Inc. 2014. Anatomy, physiology, and Pathophysiology of pain. 9–27

Sisignano M, Rice ASC, Geisslinger G. 2025. Topical Analgesics: Pharmacology and Clinical Applications. Anesthesiology. 143(5): 1371-1381. doi: 10.1097/ALN.0000000000005579.

Sokeng, S. D., Talla, E., Sakava, P., Fokam Tagne, M. A., Henoumont, C., Sophie, L. and TchuenguemFohouo, F. N. 2020. Anti-inflammatory and analgesic effect of arachic acid ethyl ester isolated from propolis. BioMed Research International. 2020(1): 8797284

Suttisuwan, R., Phunpruch, S., Saisavoey, T., Sangtanoo, P., Thongchul, N., &Karnchanatat, A. 2019. Isolation and characterization of anti-inflammatory peptides derived from trypsin hydrolysis of microalgae protein (Synechococcus sp. VDW). Food Biotechnol. 33: 303-324. https://doi.org/10.1080/08905436. 2019.1673171.

Takeda M, Sashide Y. 2025. Pain Management with Natural Products: Neurophysiological Insights. Int J Mol Sci. 26(13): 6305. doi: 10.3390/ijms26136305.

Tjølsen, A., Berge, O.G., Hunskaar, S., Rosland, J.H. and Hole, K. 1992. The formalin test: an evaluation of the method. Pain, 51(1): 5-17.

Ugwah-Oguejiofor, C., Adegboyega, A., Salubi, C., Asomadu, R., Adebisi, I., Oladehinde, T., Apata, J., Salihu, M., Agu, S., Esiaba, I. and Johnson, T., 2025. Computational evaluation of Khayaivorensis against plasmodium falciparum aminopeptidase N (PfM1AP) enzyme: Molecular docking, simulation and ADMET studies. Results in Chemistry. *14*: 102072.

Uritu, C. M., Mihai, C. T., Stanciu, G. D., Dodi, G., Alexa-Stratulat, T., Luca, A. and Tamba, B. I. 2018. Medicinal plants of the family Lamiaceae in pain therapy: A review. Pain Research and Management, 2018(1): 7801543

Vassallo, A., De Tommasi, N., Merfort, I., Sanogo, R., Severino, L., Pelin, M., Della Loggia, R., Tubaro, A. and Sosa, S., 2013. Steroids with anti-inflammatory activity from VernonianigritianaOliv. & Hiern. Phytochemistry, 96: 288-298.

Wang, J., Xu, D., Shen, L., Zhou, J., Lv, X., Ma, H., & Duan, J. 2021. Anti-inflammatory and analgesic actions of bufotenine through inhibiting lipid metabolism pathway. Biomedicine & Pharmacotherapy, 140: 111749.

Winter, C.A., Risley, E.A. and Nuss, G.W., 1962. Carrageenin-induced edema in hind paw of the rat as an assay for antiinflammatory drugs. Proceedings of the society for experimental biology and medicine, 111(3): 544-547.

World Health Organization 2012. WHO guidelines on the pharmacological treatment of persisting pain in children with medical illnesses. World Health Organization. Geneva. Accessed 2nd June 2025.

Yam, M.F., Loh, Y.C., Tan, C.S., Khadijah Adam, S., Abdul Manan, N., Basir, R. 2018. General Pathways of Pain Sensation and the Major Neurotransmitters Involved in Pain Regulation. Int J Mol Sci. 19(8): 2164. doi: 10.3390/ijms19082164.

Yusof, H. M., Ali, N. M., Yeap, S. K., Ho, W. Y., Beh, B. K., Koh, S. P., ... &Alitheen, N. B. 2019. Anti-inflammatory, analgesic, and acute, toxicity effects of fermented soybean. BMC Complementary and alternative medicine, 19(1): 1-7.

Zhu, Z.Z., Ma, K.J., Ran, X., Zhang, H., Zheng, C.J., Han, T., Zhang, Q.Y. and Qin, L.P. 2011. Analgesic, anti-inflammatory and antipyretic activities of the petroleum ether fraction from the ethanol extract of *Desmodium podocarpum*. J. Ethnopharmacol, 133(3): 1126-1131.

Supplementary table 1

S/N	Ligand Name	PubChem ID	Docking Score (kcal/mol)	
			6GPS	5COX
1.	Lunamarin	442922	-5.7	-6.0
2.	Naringin	442428	-6.4	-7.3
3.	**Ouabain**	**439501**	**-6.9**	-5.4
4.	Flavan-3-ol	3707243	-6.0	-5.8
5.	Naringenin	439246	-6.5	-7.0
6.	Spartein	644020	-5.4	-4.8
7.	**Rutin**	**5280805**	**-7.7**	**-9.4**
8.	**Hesperidin**	**10621**	**-6.9**	**-7.9**
9.	**Kaempferol**	**5280863**	**-7.9**	-6.4
10.	Epicatechin	72276	-6.9	**-7.5**
11.	Phytic-acid	890	-4.0	**-7.5**
12.	Oxalate	71081	-2.8	-4.0
13.	**Catechin**	**9064**	**-7.1**	**-7.3**
14.	Sapogenin	21139920	-5.1	-4.0
15.	Celecoxib	2662	-5.5	-6.4

Note: Top ranking compounds in red font

Access this Article in Online

Website: www.ijcrcps.com

Subject: Ethnopharmacology

Quick Response Code

DOI: 10.22192/ijcrcps.2026.13.02.003

How to cite this article:
Iyabo Mobolawa Adebisi, Aliyu Hamidu Ahmed, Boniface Clement Gomo, Sunday Joseph Fajobi, Taiwo Oladehinde, Samuel Jacob Bunu. (2026). *In-vivo* anti-nociceptive and anti-inflammatory potentials and molecular docking evaluation of chemical constituents of *Dioscorea praehensilis* targeting Cyclooxygenase-2 and chemokine receptor type 2 inhibition. Int. J. Curr. Res. Chem. Pharm. Sci. 13(2): 20-47. DOI: http://dx.doi.org/10.22192/ijcrcps.2026.13.02.003

